Noname manuscript No.
(will be inserted by the editor)

A solution procedure for constrained eigenvalue problems and its application within the structural finite-element code NOSA-ITACA

Margherita Porcelli · Vincenzo Binante · Maria Girardi · Cristina Padovani · Giuseppe Pasquinelli

Received: date / Accepted: date

Abstract The paper presents an efficient and reliable implementation of numerical methods for constrained generalized eigenvalue problems, specialized for the modal analysis of linear elastic structures in a finite-element setting. The implementation, which takes into account the sparsity of the stiffness and mass matrices and the features of master-slave constraints, is based on open-source packages embedded in the finite-element code NOSA-ITACA. Numerical tests on historical building are performed, with the aims of calculating their vibration frequencies and mode shape vectors, comparing them to the results of a general purpose commercial code and assessing the accuracy of the tool developed.

Keywords Eigenvalues · Finite-element software · Multipoint constraints

1 Introduction

In the absence of dumping, the free vibrations of a linear elastic structure discretized into finite-elements are governed by the equation

$$M\ddot{u} + Ku = 0, \tag{1}$$

where u is the displacement vector, which belongs to $\mathbb{R}^n$ and depends on time t, $\ddot{u}$ is the second-derivative of u with respect to t, and K and $M \in \mathbb{R}^{n\times n}$ are the

M. Porcelli
Dipartimento di Matematica, Università di Bologna
Piazza di Porta S. Donato 5, 40127 Bologna, Italia
Tel.: +39 051 2094423
Fax: +39 051 2094490
E-mail: margherita.porcelli@unibo.it

M. Porcelli · V. Binante · M. Girardi · C. Padovani · G. Pasquinelli
Istituto di Scienza e Tecnologie dell'Informazione Alessandro Faedo
ISTI-CNR, Via G. Moruzzi 1, 56124 Pisa, Italia

stiffness and mass matrices of the finite-element assemblage. K is symmetric and positive semidefinite; M is symmetric and positive definite; and both are banded with bandwidth depending on the numbering of the finite-element nodal points. Displacements u_i are also called degrees of freedom; the integer n is the total number of degrees of freedom of the system and is generally very large, since it depends on the level of discretization of the problem. By assuming that

$$u = \phi \sin(\omega t), \tag{2}$$

and applying the modal superposition [6], equation (1) is transformed into the generalized eigenvalue problem

$$K\,\phi = \omega^2\, M\,\phi. \tag{3}$$

In (2), ϕ is a vector of $\mathbb{R}^n$ and ω is a real scalar.

Modal analysis of a structure consists of determining the eigenvalues ω_i^2 and the eigenvectors ϕ_i of (3) that represent the natural frequencies, or eigenfrequencies (rad/sec) squared, of the structure and the corresponding mode shape vectors, or eigenmodes, respectively. Together with the natural frequencies, the mode shapes give many qualitative information on the structure deformations under dynamic loads. Besides, if a seismic analysis is required, they allow determining the conventional loads to be applied to the model, in order to simulate the effects of an earthquake in accordance to regulations [9].

In the field of structural finite-element analysis, constraints enforce certain relations between degrees of freedom. A simple example of constraints is the imposition of Dirichlet boundary conditions, which usually consists of setting certain degrees of freedom to some known value (most commonly zero). This kind of constraint is referred to as a *single-point* or *fixed* constraint and is expressed in the form

$$u_i = 0, \tag{4}$$

for some i ranging from 1 to n.

A further degree of complexity involves *multipoint constraints* which relate more than one degree of freedom, including interface element surfaces and contact conditions. Among linear multipoint constraints, a special role is played by the so called *master-slave* constraints [11]. A master-slave constraint is a condition imposed such that the displacement of a node (called the slave) depends linearly on the displacement of another node (called the master). Master-slave constraints may link the displacements of a slave node in different directions to different master nodes. Master-slave constraints can be expressed as follows: there exist subsets

$$I_S \subset \{1,\dots,n\} \quad \text{and} \quad I_{M_s} \subset \{1,\dots,n\} \setminus I_S \tag{5}$$

such that

$$u_s = \sum_{m \in I_{M_s}} c_{sm} u_m, \quad s \in I_S, m \in I_{M_s}. \tag{6}$$

u_s is the slave (or tied) degree of freedom whereas u_m are the master (or guide) degrees of freedom, and c_{sm} are real coefficients. These constraints, also known as mutual constraints, or tying relations, are crucial, for instance, in modelling the contact interaction between masonry buildings and reinforcements [15], [36].

In view of (2), fixed constraints (4) and master-slave relations of type (6) assigned to displacement u can be expressed in terms of vector ϕ as follows

$$T\phi = 0, \tag{7}$$

with $T \in \mathbb{R}^{m\times n}$ and $m \ll n$. In the considered applications, matrix K turns out to be positive definite on the null subspace of $\mathbb{R}^n$ defined by conditions (7).

In this paper, we focus on the problem of finding the $p \ll n$ smallest eigenpairs of the generalized eigenvalue problem (3) with the constraints (7) and propose a solution procedure which takes into account both the sparsity of the matrices and the features of master-slave constraints.

In Section 2 we introduce a null space projection like procedure for solving generalized eigenvalue problems with linear constraints. In Section 3, the procedure is adapted to the solution of the eigenvalue problem (3) with constraints (7), expressed in terms of fixed and master-slave degrees of freedom, and the master-slave relations are used to obtain a basis of the null space of T.

Section 4 deals with implementation of the proposed solution procedure through the applications of open-source packages embedded in the finite-element code NOSA-ITACA, which have been developed within the framework of a research project funded by the Region of Tuscany [30]. This wide-ranging project is aimed at assessing the static safety and seismic vulnerability of masonry constructions of historical interest, as well as modelling possible strengthening interventions.

Section 5 is then devoted to numerical tests. In particular, the NOSA-ITACA code is applied to three historical buildings in order to calculate their natural mode shapes and frequencies, the results of which are then compared to the quantities calculated via the commercial code Marc [33].

2 The constrained eigenvalue problem

Consider the following linearly constrained generalized eigenvalue problem

$$A\,x = \lambda\,B\,x \quad \text{subject to} \;\; Cx = 0, \tag{8}$$

where A and B are positive semidefinite sparse and symmetric matrices belonging to $\mathbb{R}^{n\times n}$, $C \in \mathbb{R}^{m\times n}$ is a sparse full row rank matrix, and A is positive definite on the null space $Null(C)$ of C. The constraint can be imposed by suitably transforming this constrained problem into a modified unconstrained eigenvalue problem and then solving it via a known strategy for unconstrained problems [12].

A possible transformation consists of projecting the eigenvalue problem into the constraint space by explicitly constructing a basis for the null space of C. Let $Z \in \mathbb{R}^{n\times(n-m)}$ be a matrix whose columns span the null space of C and for $x \in Null(C)$, let $y \in \mathbb{R}^{n-m}$ be such that $x = Zy$; we thus obtain the equivalent unconstrained formulation of problem (8) as

$$(Z^T AZ)\, y = \lambda\, (Z^T BZ)\, y, \tag{9}$$

in the subspace $Null(C)$ (see [16, Section 12.6.1]). Remarkably, the symmetry and positive definiteness of the problem are preserved, and the dimension of the problem is reduced from n to the null space dimension $(n - m)$. On the other hand, forming the matrices $(Z^T AZ)$ and $(Z^T BZ)$ might compromise their sparsity.

Computing a basis Z for $Null(C)$ can be accomplished by calculating a rank-revealing factorization of C, as suggested by the following Proposition [14, Section 6.8.1].

Proposition 1 *Let $C \in \mathbb{R}^{m\times n}$ be a full row rank matrix and let $C = GH$ be a rank-revealing factorization, i.e. let $G \in \mathbb{R}^{m\times m}, H \in \mathbb{R}^{m\times n}$ with $rank(G) = rank(H) = m$. Moreover, let H be partitioned as $H = [H_m\ H_{n-m}]$ with $H_m \in \mathbb{R}^{m\times m}$ non singular and $H_{n-m} \in \mathbb{R}^{m\times(n-m)}$. Then, the columns of the matrix $Z \in \mathbb{R}^{n\times(n-m)}$ given by*

$$Z = \begin{bmatrix} -H_m^{-1} H_{n-m} \\ I_{n-m} \end{bmatrix} \tag{10}$$

form a basis for $Null(C)$.

One example of rank-revealing factorization is represented by the LU factorization. Assuming that the LU factorization of C with complete pivoting has been computed, that is C is factorized as

$$C = \tilde{P} L U P^T,$$

where $P, \tilde{P}$ are row permutation matrices, and

$$L = \begin{pmatrix} L_{11} \\ L_{12} \end{pmatrix},\ U = \begin{pmatrix} U_{11}\ U_{21} \end{pmatrix},$$

with $L_{11}, U_{11} \in \mathbb{R}^{m\times m}$ nonsingular (lower and upper triangular). Then the matrices G and H of Proposition 1 are given by

$$G = \tilde{P} L, \quad H = U P^T,$$

which gives the following basis for $Null(C)$

$$Z = P \begin{bmatrix} -U_{11}^{-1} U_{12} \\ I_{n-m} \end{bmatrix}.$$

A further more stable way to compute an orthonormal basis Z for $Null(C)$ is by using the rank-revealing factorization $C = GH$ associated with complete

orthogonal factorization. Starting from the QR factorization of C and using a strategy based on Householder transformations [14, Section 5.5.4], one can compute the following complete orthogonal factorization of C

$$CP = Q_m \left(\bar{R}\ 0 \right) V^T P^T,$$

where $Q_m \in \mathbb{R}^{m\times m}$ corresponds to the first m columns of the orthogonal factor Q, $\bar{R} \in \mathbb{R}^{m\times m}$ is upper triangle, $V \in \mathbb{R}^{n\times n}$ and P is a row permutation. Then, the rank-revealing factors G, H are given by

$$G = Q_m \text{ and } H = \left(\bar{R}\ 0 \right) V^T P^T.$$

Now, let $\bar{V} = PV \in \mathbb{R}^{n\times n}$, $\bar{V}$ is orthogonal and satisfies

$$H\bar{V} = \left(\bar{R}\ 0 \right) \bar{V}^T \bar{V} = \left(\bar{R}\ 0 \right),$$

which shows that the last $(n-m)$ columns of $\bar{V}$, denoted by Z are orthogonal to H and hence form an orthonormal basis for $Null(C)$.

An alternative transformation of problem (8) consists of considering the associated optimality system, that is, the following augmented eigenproblem

$$\begin{bmatrix} A & C^T \\ C & 0 \end{bmatrix} \begin{bmatrix} x \\ \mu \end{bmatrix} = \lambda \begin{bmatrix} B & 0 \\ 0 & 0 \end{bmatrix} \begin{bmatrix} x \\ \mu \end{bmatrix}, \tag{11}$$

where $\mu \in \mathbb{R}^m$ represents the Lagrange multipliers. In this case the dimension of the problem increases by m with respect to the original one; the sparsity pattern of the involved matrices is preserved but in general eigenproblem (11) is not positive definite [3,4].

In this paper we focus on transformation (9) and will adopt the *null space projection procedure* [17], meaning a strategy that first converts the original problem (8) into the projected problem (9) and then applies a standard method for symmetric positive definite eigenproblems (see Section 4.1).

3 Solving the generalized eigenvalue problem with master-slave constraints

In this section we focus on modal analysis of elastic structures discretized with finite-elements, which involves solving the large-size eigenvalue problem (3) with constraints (7) expressing the fixed and master-slave relations. In finite-element structural analysis, the main approach adopted to take master-slave constraints into account is the master-slave method, consisting of explicitly eliminating the slave and fixed degrees of freedom and then solving the problem only for the master and unconstrained displacements. Further approaches comprise the penalty method and the Lagrange multiplier method (see [3], [10], [11, Chapter 8] and [27]).

Here, we adopt the null space projection approach based on Proposition 1 of the previous section. A motivation for the use of this approach is that, due to the special constraint structure, the computation of a rank-revealing factorization $T = GH$ of the constraint matrix T does not involve any LU or QR factorization necessary in the general case and, furthermore, there is no need of inverting matrices while forming the basis Z in (10) for $Null(T)$.

In this section, first, we provide a basis for the null space of T whose construction is strongly dependent on the master-slave relations (7), then we show that the projected problem obtained using this basis has a very favorable sparsity structure which is the reason for the implementation choices presented in Section 4.

Selection of the master and slave degrees of freedom follows some specific rules and this imparts a special structure to matrix $T \in \mathbb{R}^{m\times n}$ in (7): if a degree of freedom is master, it cannot be a slave and vice versa; a master can guide more than one slave degree of freedom, and a slave degree of freedom cannot appear in different master-slave relations (see (6)). Moreover, generally, master or slaves degrees of freedom cannot be a fixed degree of freedom. In the sporadic cases when a master degree of freedom is fixed, it can be explicitly eliminated, so that we can assume that T has full row rank.

Let us define the following index sets and the corresponding cardinality:

$$
\begin{aligned}
I_F &= \{i \in \{1,\dots n\} \mid u_i \text{ is a fixed degree of freedom}\},\ n_F = |I_F| \\
I_S &= \{i \in \{1,\dots n\} \mid u_i \text{ is a slave degree of freedom}\},\ n_S = |I_S| \\
I_M &= \{i \in \{1,\dots n\} \mid u_i \text{ is a master degree of freedom}\},\ n_M = |I_M| \\
I_U &= \{i \in \{1,\dots n\} \mid u_i \text{ is an unconstrained degree of freedom}\},\ n_U = |I_U|.
\end{aligned}
$$

By construction, the four sets are disjoint and their union gives the whole set of degrees of freedom so that $m = n_F + n_S$ and $n = n_F + n_S + n_M + n_U$. Note that $I_M = \bigcup_{s\in I_S} I_{M_s}$ with I_{M_s} in (5).

Assuming that matrix T columns are reordered so that they correspond to degrees of freedom in the order fixed-slave-master-unconstrained and assuming that $i \le j$ for all $i \in I_F$ and $j \in I_S$, we can express matrix T as

$$T = [T_{I_F}\ T_{I_S}\ T_{I_M}\ T_{I_U}],$$

where $T_{I_F} \in \mathbb{R}^{m\times n_F}, T_{I_S} \in \mathbb{R}^{m\times n_s}, T_{I_M} \in \mathbb{R}^{m\times n_M}, T_{I_U} \in \mathbb{R}^{m\times n_U}$ and the first n_F rows correspond to fixed constraints.

Due to the definition of fixed (4) and master-slave (6) constraints, matrix $[T_{I_F} T_{I_S}]$ is the identity matrix $I_m \in \mathbb{R}^{m\times m}$, block T_{I_U} is the null block $\mathbf{0}_{m,n_U}$, and block T_{I_M} takes the form

$$T_{I_M} = \begin{bmatrix} \mathbf{0}_{n_F,n_M} \\ \hat{T} \end{bmatrix} \in \mathbb{R}^{n_S\times n_M},$$

where $\hat{T}$ contains the nonzero coefficients $-c_{sm}$ from (6). Summarizing then, the constraint matrix has the following sparse block structure

$$\begin{array}{c} \\ n_F \\ n_S \end{array} \begin{array}{c} \begin{array}{cccc} n_F & n_S & n_M & n_U \end{array} \\ \begin{pmatrix} I_{n_F} & 0 & 0 & 0 \\ 0 & I_{n_S} & \hat{T} & 0 \end{pmatrix} \end{array}.$$

Due to this special structure, a rank-revealing factorization for T is simply given by $T = GH$ with $G = I_m, H = T$ and submatrices H_m, H_{n-m} in (10) are

$$H_m = [T_{I_F}\ T_{I_S}] \text{ and } H_{n-m} = [T_{I_M}\ T_{I_U}].$$

Consequently, a basis Z of the null space of T is trivially given by

$$Z = \begin{bmatrix} -[T_{I_M}\ \mathbf{0}_{m,n_U}] \\ I_{n-m} \end{bmatrix}. \tag{12}$$

Clearly the construction of Z in (12) is straightforward and, in addition, it is generally very sparse. In fact, in the applications the number of master per slave degrees of freedom varies from 1 to 3 so that block $\hat{T}$ in T_{I_M} itself is also very sparse.

Note that if only fixed constraints are present (i.e. $I_S = I_M = \emptyset$), then solving problem (3)-(7) simply requires eliminating the rows and columns (symmetrically) corresponding to fixed degrees of freedom in the matrices K and M.

In the next proposition we prove that if K, M are sparse matrices, then the projected matrices $Z^T KZ, Z^T MZ$, with Z in the form (12) are still sparse.

Proposition 2 *Let $A \in \mathbb{R}^{n\times n}$ be partitioned as*

$$\begin{array}{c} \\ m \\ (n-m) \end{array} \begin{array}{c} \begin{array}{cc} m & (n-m) \end{array} \\ \begin{pmatrix} A_{11} & A_{12} \\ A_{21} & A_{22} \end{pmatrix} \end{array}.$$

Let $Z \in \mathbb{R}^{n\times(n-m)}$ be expressed in the form

$$Z = \begin{bmatrix} Z_1 \\ I_{n-m} \end{bmatrix} \quad \text{with } Z_1 \in \mathbb{R}^{m\times(n-m)} \text{ s.t. } Z_1 = \begin{bmatrix} W\ 0 \end{bmatrix},\ W \in \mathbb{R}^{m\times n_m}.$$

Then

$$nnz(Z^T AZ) \le nnz(A_{22}) + (n_m)^2 + 2n_m(n-m-n_m), \tag{13}$$

where $nnz(\cdot)$ denote the number of nonzeros.

Proof Computing the direct block product $Z^T AZ$ we get

$$\begin{aligned} Z^T AZ &= \begin{bmatrix} Z_1^T\ I_{n-m} \end{bmatrix} \begin{bmatrix} A_{11}\ A_{12} \\ A_{21}\ A_{22} \end{bmatrix} \begin{bmatrix} Z_1 \\ I_{n-m} \end{bmatrix} \\ &= \begin{bmatrix} Z_1^T A_{11} + A_{21}\ Z_1^T A_{12} + A_{22} \end{bmatrix} \begin{bmatrix} Z_1 \\ I_{n-m} \end{bmatrix} \\ &= \begin{bmatrix} Z_1^T A_{11} Z_1 + A_{21} Z_1 + Z_1^T A_{12} + A_{22} \end{bmatrix}. \end{aligned}$$

Since $Z_1 = \begin{bmatrix} W & 0 \end{bmatrix}$, we have

$$A_{21}Z_1 = A_{21}\begin{bmatrix} W & 0 \end{bmatrix}^T = \begin{bmatrix} A_{21}W & 0 \end{bmatrix}$$

and

$$Z_1^T A_{12} = \left(A_{12}^T Z_1\right)^T = \begin{bmatrix} A_{12}^T W & 0 \end{bmatrix} = \begin{bmatrix} W^T A_{12} \\ 0 \end{bmatrix}$$

and

$$Z_1^T A_{11} Z_1 = Z_1^T \begin{bmatrix} A_{11}W & 0 \end{bmatrix} = \begin{bmatrix} W^T \\ 0 \end{bmatrix} \begin{bmatrix} A_{11}W & 0 \end{bmatrix} = \begin{bmatrix} W^T A_{11} W & 0 \\ 0 & 0 \end{bmatrix}$$

Then $Z^T AZ = Q + A_{22}$ with $Q \in \mathbb{R}^{(n-m)\times(n-m)}$ given by

$$\begin{array}{c} \\ n_m \\ (n-m-n_m) \end{array} \begin{array}{c} \begin{array}{cc} n_m & (n-m-n_m) \end{array} \\ \begin{pmatrix} * & * \\ * & 0 \end{pmatrix} \end{array}$$

where $'*'$ denotes the possibly nonzero blocks. Thus, $nnz(Z^T AZ) \leq nnz(A_{22}) + n_m^2 + 2n_m(n-m-n_m)$.

□

Remarkably, the inequality (13) implies that in the projected matrices $Z^T KZ$, $Z^T MZ$, with Z in the form (12), only at most n_M rows and n_M columns might fill-in where $n_M \ll n$ is the number of master degrees of freedom.

4 Implementation within the NOSA-ITACA code

In this section we describe the implementation of the procedure for solving the constrained eigenvalue problem (3)-(7) in the NOSA-ITACA code. NOSA-ITACA is a freeware code resulting from integration of the Fortran finite-element code NOSA [29] into the open-source SALOME platform [40]. It has been developed within the framework of the project "Tools for modelling and assessing the structural behaviour of ancient constructions: the NOSA-ITACA code", funded by the Region of Tuscany in the period 2011-2013 [30]. The main goal of the project has been to develop a new tool, the NOSA-ITACA code, for the static and dynamic analysis of masonry buildings of historical interest. The code models masonry as a nonlinear elastic material with zero tensile strength and bounded compressive strength [29]. Although the constitutive equation adopted for masonry is nonlinear, the modal analysis, which is based on the assumption that the materials constituting the construction are linear elastic, furnishes important qualitative information on the dynamic behavior of masonry structures and thereby allows for assessing their seismic vulnerability in light of Italian and European regulations [9].

4.1 Iterative eigensolvers

The body of literature on numerical methods for solving large constrained eigenvalue problems (8) is not very extensive [12],[16, Section 12.6.1], [17,27]. On the other hand, many algorithms have been proposed for unconstrained eigenvalue problems of the form $Ax = \lambda Bx$ yielding to the development in recent years of robust and computationally efficient schemes [38,43] and corresponding software packages [18,35]. The most promising approaches for the important class of symmetric positive definite matrices include the implicitly restarted Arnoldi method (equivalent to the Lanczos technique for this type of matrices) [25,26], the recently proposed Jacobi-Davidson algorithm [8,31, 41] and schemes based on preconditioned conjugate gradient minimization of the Rayleigh quotient [1,5,13,22,23]. All these methods seem to outperform the widely used subspace iteration scheme [32].

Regarding the implementation of the main algorithms, an exhaustive survey of freely available software tools for numerical solution of large-sparse eigenvalue problems can be found in [18]. The survey includes a list of libraries, programs or subroutines and brief descriptions of the algorithms. Some recent papers have moreover compared the different methods/solvers and provided extensive numerical examples on applicative problems [1,5,24].

One of the most popular eigensolvers, ARPACK, has been chosen here for solving the reduced problem arising in the null space approach due to its efficiency and robustness [25,26]. In particular, its reliability has been widely demonstrated in the solution of real, large problems, for instance in image reconstruction, molecular dynamics simulations, iterative determination of vibrational energy levels, large-scale electromagnetic eigenvalue problems, etc. [2]. All these features make it well-suited for use in the framework of the NOSA-ITACA code.

ARPACK provides a Fortran 77 implementation of the Implicitly Restarted Arnoldi method, for both real and complex arithmetic. It can be used for both standard and generalized problems and for both symmetric and nonsymmetric problems. In the symmetric case, Lanczos with full reorthogonalization is used instead of Arnoldi. The algorithm is based on the classical Arnoldi/Lanczos factorization combined with spectral techniques to improve the convergence of basic methods. To overcome intractable storage and computational requirements in the standard Arnoldi (or Lanczos) method, restarting techniques have been developed and Implicit restarting is a variant of such techniques. The resulting method may thus be viewed as a truncated form of the implicitly shifted QR-algorithm that is appropriate for large problems. For detailed information on the algorithm implemented in ARPACK, we refer the reader to the users' guide [26].

4.2 Implementation issues

We implemented the null-space projection procedure flowcharted in Figure 1 to solve the constrained eigenvalue problem (3)-(7). Firstly the constrained problem is converted into the unconstrained problem

$$\tilde{K}\, y = \omega^2\, \tilde{M}\, y, \tag{14}$$

where

$$\tilde{K} = Z^T K Z, \quad \tilde{M} = Z^T M Z, \tag{15}$$

with the basis Z in (12) and $y \in \mathbb{R}^{n-m}$; secondly this reduced problem is solved using ARPACK; and lastly the eigenvectors are expanded back to the full space.

Due to the sparsity structure of the stiffness and mass matrices, known in theory from Proposition 2 and that will be verified in practice in Section 5, we stored the assembled matrices in a compressed sparse format and we used the Fortran routines of the SPARSKIT package [39]. SPARSKIT provides many efficient routines for manipulating and working with sparse matrices. Specifically, we used the routines for converting data structures and for general algebraic operations (e.g. matrix-vector products) contained in the BLASSM module.

Moreover, ARPACK has a reverse communication interface that requires the user to supply a routine for performing the matrix-vector multiplication with $\tilde{M}$ and $\tilde{K}$ and a linear system solver. Clearly, its efficiency depends upon these routines. We used SPARSKIT for the products and chose to solve the systems by iterative methods imposing a stringent tolerance in order to obtain accurate eigenvalue, as suggested in [26].

All the packages were run using the default parameters. We moreover selected the *Shift-invert mode* with null pole σ, for which, ARPACK requires the action

$$w \leftarrow (\tilde{K} - \sigma\tilde{M})^{-1}\tilde{M}v, \quad \sigma = 0,$$

to be supplied. Therefore, a sequence of symmetric, positive definite linear systems of the form

$$\tilde{K}w = b_k,\ k = 1, 2 \ldots \tag{16}$$

in which the coefficient matrix is constant but the right-hand side $b_k \in \mathbb{R}^{n-m}$ varies, has to be solved. For solving the sequence (16), we used the Conjugate Gradient method that is the Krylov subspace method best-suited for solving large symmetric positive definite systems. Its convergence rate depends on the condition number of the matrix $\tilde{K}$ and then, it is widely recognized that preconditioning is a critical ingredient to reduce the condition number, and hence improve the performance of the iteration [19, 21]. We then considered the ICFS-preconditioner that is based on the well-known Incomplete Cholesky Factorization with limited memory proposed in [28] for positive definite or indefinite systems. The ICFS-preconditioner has the favorable property to control the amount of additional memory and then, there is no need to specify

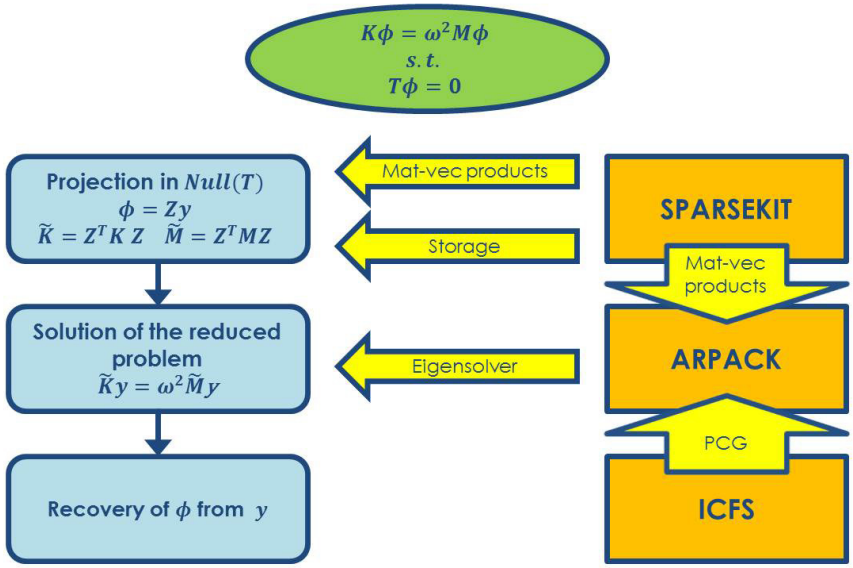

Fig. 1 *Flowchart of the implemented null-space projection procedure to solve the constrained problem (3)-(7).*

a drop tolerance. Note that the preconditioner has to be computed only ones for the matrix $\tilde{K}$ and then is reused for the solution for each kth systems of the sequence (16).

Concerning the third phase, by taking the connectivity of the mesh and matrix Z in (12) into account, it is possible to calculate the eigenvectors ϕ of (3)-(7) from the eigenvectors y of (14).

5 Test cases and experiments

In this section, the NOSA-ITACA code is used to calculate the frequencies and mode shapes of three historical Italian buildings: the Clock Tower and the Church of San Francesco in Lucca, and the Voltone in Livorno, shown in the Figures 2, 3 and 4, respectively.

The Clock Tower, dating back to the 13th century, is one of the numerous historical buildings in Lucca. This is Lucca's highest tower, located on its main street, and has contained a clock since 1390. In the model, the Clock Tower has been discretized into 11449 8-node brick and beam elements as presented in Figure 2; only fixed constraints are considered. The Church of San Francesco, dating back to the 13th century, is a typical Franciscan masonry building with one nave, about 70 m long, 16 m wide and 19 m high. A portion of the Church has been discretized into 15403 8-node brick, beam and thick shell elements as shown in Figure 3. The roof is modelled with beam elements connected to the walls via multipoint constraints. The Voltone is a large vaulted masonry

structure located beneath the Piazza della Repubblica in Livorno; its finite-element discretization in given in Figure 4. In this case, both beam and thick shell elements have been used and master-slave constraints imposed to model the connection between the vault and the longitudinal walls.

The details on discretization and constraint type are summarized in Table 1 for each test case. In particular, p is the number of frequencies sought, m denotes the number of fixed and slave degrees of freedom, $\tilde{n} = n - m$ is the dimension of the reduced problem (14) and Δ is the bandwidth of K and M.

Table 1 Details on the discretization of the test cases.

	p	n	n_F	n_S	n_M	m	$\tilde{n}$	Δ
Clock Tower	10	46164	320	0	0	320	45844	1239
Church of San Francesco	10	61881	2662	54	54	2716	59165	11769
Voltone	30	44370	3864	1932	1932	5796	38574	1050

Let us now consider Figures 5-7. Figure 5 shows a plot of the sparsity pattern of the projected matrices $\tilde{K}$ and $\tilde{M}$ for the Clock Tower (only fixed constraints are present). Figures 6 and 7 instead, for the other two test cases, plot the sparsity pattern of the assembled stiffness matrix K (on the left) and the corresponding projected matrix $\tilde{K}$ (on the right). The plots show that the fill-in in the projected matrices is low, that is, the reduced matrices remain sparse even though the bandwidth may become larger, as stated by Proposition 2. The graphics have been obtained using the *spy* Matlab command.

The natural mode shapes and frequencies $\nu_i = \omega_i/2\pi$ (Hz) of the three historical buildings have been calculated with NOSA-ITACA. Figures 8, 9, and 10 show the mode shapes ϕ_1 and ϕ_2 for the Clock Tower and the Church of San Francesco, and the mode shapes ϕ_4 and ϕ_{21} for the Voltone.

Tables 2-4 show a comparison of the frequencies calculated via the NOSA-ITACA code with those calculated using the general purpose finite-element code Marc [33] for which we selected the Lanczos type solver. The residuals reported in the table are the 2-norms of the vectors $\tilde{K}\, z_i - \lambda_i^2\, \tilde{M}\, z_i$, with z_i and λ_i the approximations of the eigenvectors y_i and the eigenvalues ω_i calculated with NOSA-ITACA. Unfortunately, Marc does not furnish analogous quantities. The tables show that the values computed by both solvers are very similar, except for λ_9 computed for the Church of San Francesco (see Table 3). The reasons for this discrepancy are rather puzzling since the residual for this value computed by NOSA-ITACA is of the same magnitude as those for the others frequencies (of the order of 10^{-10}) . On the other hand, it is not possible to retrieve further information on the value computed by Marc, regarding neither the imposed accuracy nor estimates of the error.

Table 5 reports the CPU times for both NOSA-ITACA and Marc for the three test cases. The higher CPU times required by NOSA-ITACA (around a factor 2 if master-slave constraints are present), are probably due to the fact that, unlike Marc which uses a Cuthill-McKee algorithm [7], the current

NOSA-ITACA implementation contains no algorithms for profile reduction of matrices, that is reduction of the sum of the row bandwidths.

6 Conclusions

In this paper we have addressed the problem of finding the few smallest vibration frequencies and corresponding shape mode vectors of linear elastic structures discretized into finite-elements. We have considered the generalized eigenvalue problem (3) with the master-slave relations (7) and have surveyed the existing literature concerning its solution and the available implementations. We have then proposed a solution procedure which takes into account both the nonzero pattern of the involved matrices and the structure of the constraints. The implementation of the procedure is based on open-source packages and have been embedded into the finite-element code NOSA-ITACA. Validation tests on three historical buildings located in Tuscany heve been carried out by comparing the NOSA-ITACA results with those obtained via the commercial code Marc. The results of NOSA-ITACA are fully consistent with those of Marc, though improvements to the code in terms of CPU times could be achieved by implementing an optimizer aimed at reducing the profile of both the assembled matrices K and M and the corresponding projected ones, see e.g. [42].

The applicative impact of NOSA-ITACA enriched with the new tool for the modal analysis is significant and the code represents a valid instrument for private and public bodies operating in the field of the conservation and safeguarding of the cultural heritage, with particular application to the protection of the national architectural heritage subjected to seismic risk. Moreover, some major advantages of the described implementations, are that they can be easily employed in general finite-element codes and be included in open-source packages for the modal analysis of structures [34].

Acknowledgements This research was supported by the Region of Tuscany (Project "Tools for modelling and assessing the structural behaviour of ancient constructions: the NOSA-ITACA code", PAR-FAS 2007-2013) and by *National Group of Computing Science (GNCS-INDAM)* (GNCS 2013 Project "Strategie risolutive per sistemi lineari tipo KKT con uso di informazioni strutturali", GNCS 2013-2014 Project "Identificazione automatica dei parametri algoritmici ottimali").

References

1. P. Arbenz, U.L. Hetmaniuk, R.B. Lehoucq, R.S. Tumin, *A comparison of eigensolvers for large-scale 3D modal analysis using AMG-preconditioned iterative methods*, Int. J. Numer. Meth. Engng 2005; 64:204–236.
2. `http://www.caam.rice.edu/software/ARPACK/`.
3. C.G. Baker, R.B. Lehoucq, *Preconditioning constrained eigenvalue problems*, Linear Algebra and its Applications, Volume 431, Issues 3-4, 15 July 2009, pp. 396–408.

Fig. 2 *The Clock Tower and the finite-element mesh.*

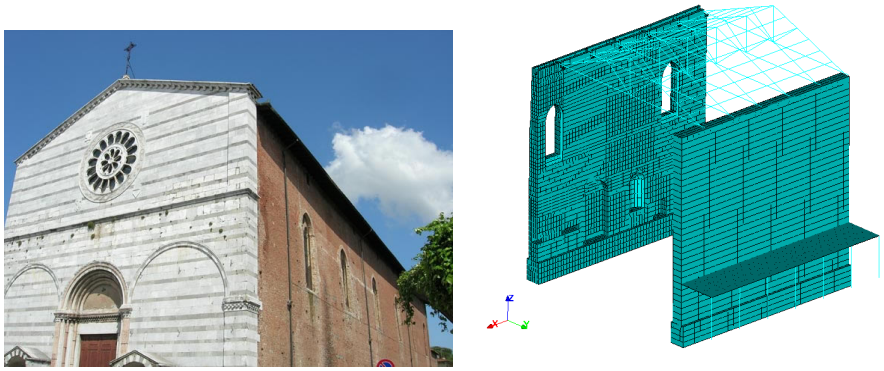

Fig. 3 *The Church of San Francesco and the finite-element discretization of a portion.*

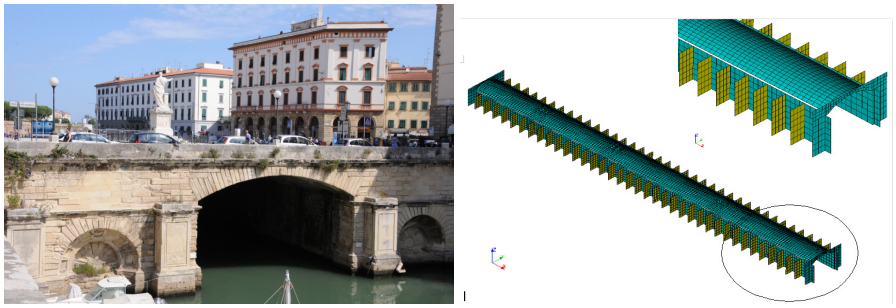

Fig. 4 *The Voltone and the finite-element mesh.*

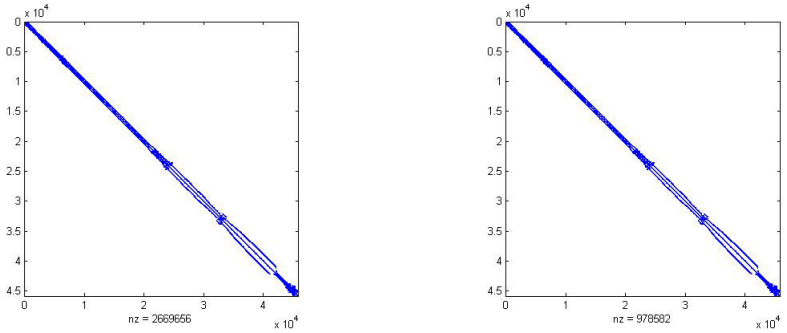

Fig. 5 *The projected stiffness and mass matrices (Clock Tower).*

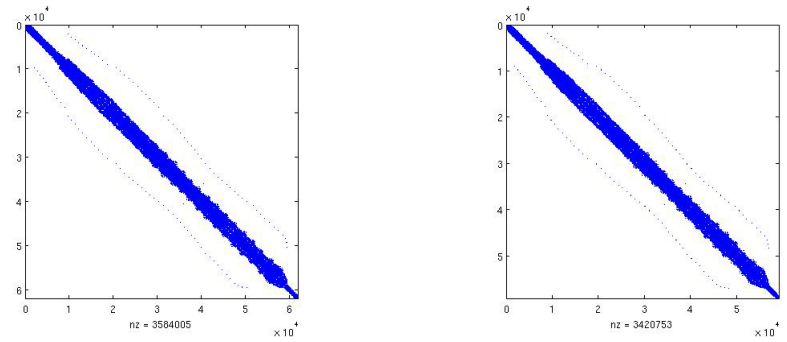

Fig. 6 *The stiffness matrix K and the projected matrix $\tilde{K}$ (Church of San Francesco).*

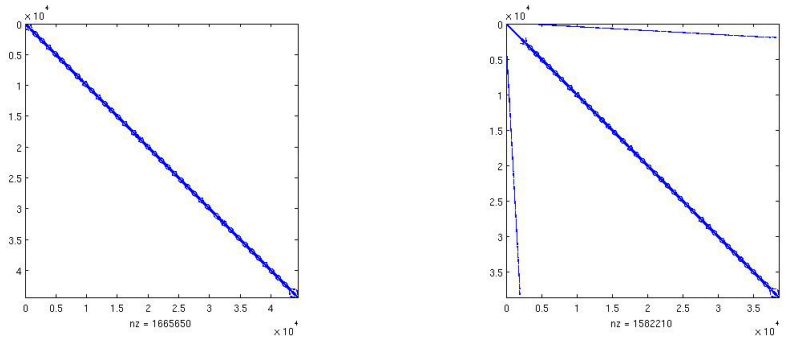

Fig. 7 *The stiffness matrix K and the projected matrix $\tilde{K}$ (Voltone).*

4. M. Bhardwaj, K. Pierson, G. Reese, T.Walsh, D. Day, K. Alvin, J. Peery, *Salinas: A scalable software for high-performance structural and solid mechanics simulation*, Proceedings of the 2002 ACM/IEEE conference on Supercomputing, p.1–19, November 16, 2002, Baltimore, Maryland.
5. L. Bergamaschi, M. Putti (2002), *Numerical Comparison of Iterative Eigensolvers for Large Sparse Symmetric Positive Definite Matrices*, Comput. Methods Appl. Mech. Engrg., 191(45):5233–5247.
6. K.J. Bathe, E. L. Wilson, *Numerical Methods in Finite Element Analysis*, Prentice-Hall, 1976.

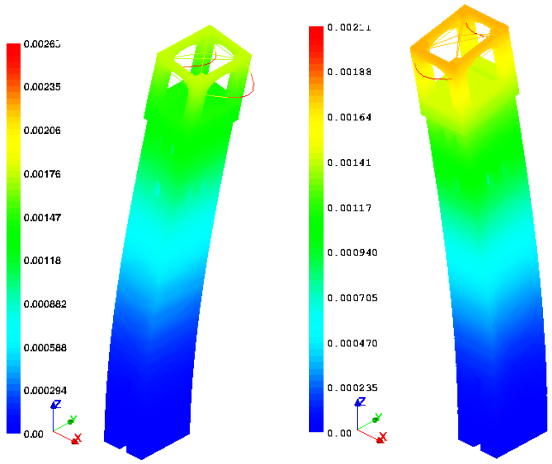

Fig. 8 *The Clock Tower, mode shape vector* ϕ_1 *corresponding to the frequency* $\nu_1 = 0.67$ *Hz (left) and mode shape vector* ϕ_2 *corresponding to the frequency* $\nu_2 = 0.89$ *Hz (right).*

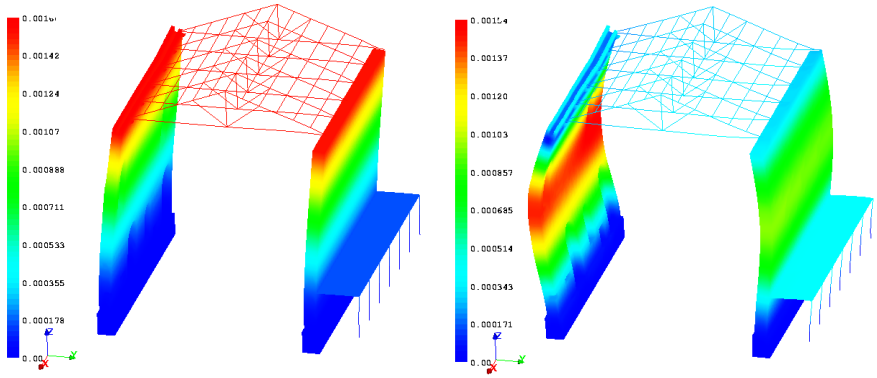

Fig. 9 *The Church of San Francesco, mode shape vector* ϕ_1 *corresponding to the frequency* $\nu_1 = 0.55$ *Hz (left) and mode shape vector* ϕ_2 *corresponding to the frequency* $\nu_2 = 2.24$ *Hz (right).*

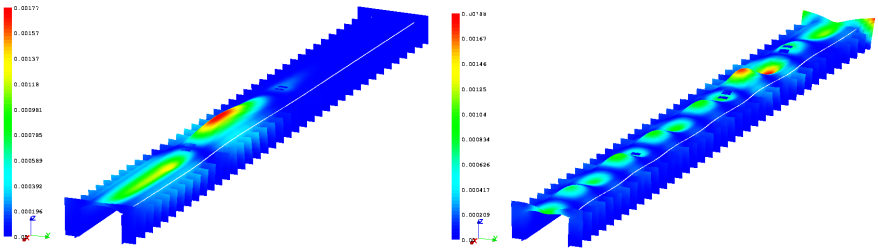

Fig. 10 *The Voltone, mode shape vector* ϕ_4 *corresponding to the frequency* $\nu_4 = 4.60$ *Hz (left) and mode shape vector* ϕ_{21} *corresponding to the frequency* $\nu_{21} = 5.96$ *Hz (right).*

Table 2 Results on the Clock Tower.

The Clock Tower			
	NOSA-ITACA		Marc
mode number	Frequencies (Hz)	Residuals	Frequencies (Hz)
1	0.67	$6.09\ 10^{-9}$	0.67
2	0.89	$6.47\ 10^{-9}$	0.89
3	1.23	$1.74\ 10^{-8}$	1.20
4	1.23	$5.90\ 10^{-9}$	1.20
5	1.23	$6.14\ 10^{-8}$	1.20
6	1.23	$3.48\ 10^{-8}$	1.20
7	2.23	$2.23\ 10^{-7}$	2.19
8	2.23	$3.93\ 10^{-8}$	2.19
9	2.23	$6.24\ 10^{-8}$	2.19
10	2.23	$1.88\ 10^{-8}$	2.19
11	3.14	$1.00\ 10^{-8}$	3.32
12	3.93	$3.14\ 10^{-8}$	3.93
13	4.12	$1.26\ 10^{-8}$	4.12

Table 3 Results on the Church of San Francesco.

The Church of San Francesco			
	NOSA-ITACA		Marc
mode number	Frequencies (Hz)	Residuals	Frequencies (Hz)
1	0.55	$5.99\ 10^{-9}$	0.55
2	2.24	$4.7\ 10^{-10}$	2.24
3	2.91	$3.15\ 10^{-10}$	2.91
4	3.16	$3.48\ 10^{-10}$	3.16
5	3.62	$3.01\ 10^{-10}$	3.62
6	5.99	$1.25\ 10^{-10}$	5.99
7	6.60	$4.00\ 10^{-10}$	6.60
8	6.61	$1.55\ 10^{-10}$	6.60
9	7.68	$8.75\ 10^{-10}$	6.62
10	7.83	$1.44\ 10^{-10}$	7.62

7. E. Cuthill, J. McKee, *Reducing the bandwidth of sparse symmetric matrices*, In Proc. 24th Nat. Conf. ACM, pages 157–172, 1969.
8. E.R. Davidson, *The iterative calculation of a few of the lowest eigenvalues and corresponding eigenvectors of large real-symmetric matrices*, Journal of Computational Physics 1975; 17:87–94.
9. D.M. 14 gennaio 2008, Norme Tecniche per le Costruzioni, G.U. 4 febbraio 2008, n. 29.
10. C. Farhat, C. Lacour, D. Rixen, *Incorporation of linear multipoint constraints in substructure based iterative solvers. Part 1: a numerically scalable algorithm*, International Journal for Numerical Methods in Engineering Volume 43, Issue 6, pages 997-1016, 1998.
11. C. Felippa, *Lectures Notes for Introduction to Finite Element Methods*, (ASEN 5007), Revised Fall 1997, http://www.colorado.edu/engineering/cas/courses.d/IFEM.d/. 6.
12. W. Gander, G.H. Golub, U. von Matt, *A constrained eigenvalue problem*, Linear Algebra and its Applications Volumes 114115, March–April 1989, Pages 815-839.
13. G. Gambolati, F. Sartoretto, P. Florian, *An orthogonal accelerated deflation technique for large symmetric eigenproblems*, Comp. Meth. Appl. Mech. Engrg. 94 (1992) 13-23.
14. Ph.E. Gill, W. Murray, M.H. Wright, *Numerical linear algebra and optimization*, Volume I, Addison-Wesley, 1991.

Table 4 Results on the Voltone.

The Voltone			
	NOSA-ITACA		Marc
mode number	Frequencies (Hz)	Residuals	Frequencies (Hz)
1	4.09	$1 \cdot 10^{-9}$	4.09
2	4.34	$5 \cdot 10^{-10}$	4.34
3	4.45	$2 \cdot 10^{-9}$	4.45
4	4.60	$9 \cdot 10^{-10}$	4.60
5	4.65	$5 \cdot 10^{-10}$	4.66
6	4.77	$3 \cdot 10^{-10}$	4.77
7	4.80	$6 \cdot 10^{-10}$	4.80
8	4.81	$2 \cdot 10^{-9}$	4.81
9	4.91	$2 \cdot 10^{-9}$	4.90
10	4.97	$5 \cdot 10^{-10}$	4.97
11	5.19	$1 \cdot 10^{-9}$	5.19
12	5.22	$7 \cdot 10^{-10}$	5.22
13	5.27	$9 \cdot 10^{-10}$	5.27
14	5.34	$1 \cdot 10^{-9}$	5.34
15	5.43	$1 \cdot 10^{-9}$	5.43
16	5.50	$5 \cdot 10^{-10}$	5.51
17	5.76	$6 \cdot 10^{-10}$	5.76
18	5.77	$8 \cdot 10^{-10}$	5.77
19	5.84	$2 \cdot 10^{-9}$	5.85
20	5.90	$2 \cdot 10^{-9}$	5.90
21	5.96	$4 \cdot 10^{-10}$	5.97
22	6.04	$1 \cdot 10^{-9}$	6.01
23	6.13	$1 \cdot 10^{-9}$	6.12
24	6.14	$6 \cdot 10^{-10}$	6.15
25	6.25	$9 \cdot 10^{-10}$	6.25
26	6.28	$3 \cdot 10^{-10}$	6.29
27	6.39	$1 \cdot 10^{-9}$	6.38
28	6.48	$5 \cdot 10^{-10}$	6.49
29	6.50	$1 \cdot 10^{-9}$	6.50
30	6.62	$5 \cdot 10^{-10}$	6.62

Table 5 CPU time of NOSA-ITACA and Marc for the three test cases.

	CPU time (sec)	
	NOSA-ITACA	Marc
The Clock Tower	105	96
Church of S. Francesco	108	56
The Voltone	43	27

15. M. Girardi, C. Padovani, G. Pasquinelli, *Numerical modelling of the static and seismic behaviour of historical buildings: the church of San Francesco in Lucca*, CC2013 - Fourteenth International Conference on Civil, Structural and Environmental Engineering Computing (Cagliari, Italy, 3-6 September 2013), Proceedings, article n. 80. B.H.V. Topping, P. Ivnyi (eds.). Civil-Comp Press, 2013.
16. G. Golub, C. Van Loan (1996), *Matrix computations*, Third edition. London, The Johns Hopkins University Press.
17. G. Golub, Z. Zhang, H. Zha, *Large sparse symmetric eigenvalue problems with homogeneous linear constraints: the Lanczos process with innerouter iterations*, Linear Algebra

and its Applications, Volume: 309, Issue: 1-3, April 15, 2000, pp. 289-306.
18. V. Hernández, J. E. Román, A. Tom ás, V. Vidal, *A Survey of Software for Sparse Eigenvalue Problems*, SLEPc Technical Report STR-6.
19. M.R. Hestenes, E. Stiefel, *Methods of Conjugate Gradients for solving linear systems*, J. Res. Natl. Bur. Stand., 49 (1952), pp. 409-436.
20. E. Hinton, D.R.J. Owen, *Finite Element Programming*, Computational Mathematics and Applications, London, Academic Press 1977.
21. C.T. Kelley, *Iterative methods for linear and nonlinear equations*, Frontiers in Applied Mathematics, SIAM, 1995.
22. A.V. Knyazev, A.L. Skorokhodov, *The preconditioned gradient-type iterative methods in a subspace for partial generalized symmetric eigenvalue problem*, SIAM J. Numer. Anal. 31 (1994) 1226–1239.
23. A.V. Knyazev, *Toward the optimal preconditioned eigensolver: locally optimal block preconditioned conjugate gradient method*, SIAM Journal on Scientific Computing 2001; 23(2):517–541.
24. R.B. Lehoucq, J.A. Scott (1996). *An Evaluation of Software for Computing Eigenvalues of Sparse Nonsymmetric Matrices*. Preprint MCS-P547-1195, Argonne National Laboratory.
25. R.B. Lehoucq, D.C. Sorensen, *Deflation techniques for an implicit restarted Arnoldi iteration*, SIAM J. Matrix Anal. Appl. 17 (1996) 789–821.
26. R.B. Lehoucq, D.C. Sorensen, C. Yang, *ARPACK Users Guide. Solution of Large Scale Eigenvalue Problem with Implicit Restarted Arnoldi Methods*, SIAM, 1998.
27. P. Lidström, P. Olsson, *On the natural vibrations of linear structures with constraints*, Journal of Sound and Vibration 301(1-2), 2007,341-354. SIAM, 1998.
28. C.J. Lin, J.J. Moré, *Incomplete Cholesky factorizations with limited memory*, SIAM J. Sci. Comput. 21, 24 (1999).
29. M. Lucchesi, C. Padovani, G. Pasquinelli, N. Zani, *Masonry constructions: mechanical models and numerical applications*, Lecture Notes in Applied and Computational Mechanics vol. 39, Springer, 2008.
30. `http://www.nosaitaca.it/en`.
31. Y. Notay, *Combination of JacobiDavidson and conjugate gradients for the partial symmetric eigenproblem*, Numerical Linear Algebra with Applications 2002; 9:2144.
32. B. Nour-Omid, B.N. Parlett, R.L. Taylor, *Lanczos versus subspace iteration for solution of eigenvalue problems*, Int. J. Numer. Meth. Engrg. 19 (1983) 859871
33. `http://www.mscsoftware.com/Products/CAE-Tools/Marc.aspx`.
34. `http://opensees.berkeley.edu/`
35. B.N. Parlett, *The software scene in the extraction of eigenvalues from sparse matrices*, SIAM J. Sci. Stat. Comput. 5 (3) (1984) 590604.
36. G. Pasquinelli, *On the modeling of the reinforcement rings in masonry buildings: an example*. Proceedings of the Third International Conference on Contact Mechanics, Contact Mechanics III, Madrid 1997.
37. Y. Saad, *Iterative methods for sparse linear systems*, (2nd edition), SIAM, 2003.
38. Y. Saad, *Numerical Methods for Large Eigenvalue Problems*, Manchester University Press, New York, 1992.
39. Y. Saad, *SPARSKIT: A basic tool kit for sparse matrix computations*, Tech. Rep. RIACS-90-20, Research Institute for Advanced Computer Science, NASA Ames Research Center,Moffet Field, CA, 1990.
40. `http://www.salome-platform.org`
41. G.L.G. Sleijpen, H.A. van der Vorst, *A Jacobi–Davidson method for linear eigenvalue problems*, SIAM J. Matrix Anal. Appl. 17 (1996) 401425.
42. S.W. Sloan, *A Fortran program for profile and wavefront reduction*, International Journal for Numerical Methods in Engineering, Vol. 28, 2651–2679, 1989.
43. D.C. Sorensen, *Numerical methods for large eigenvalue problems*, Acta Numerica, 11 (2002) 519-584.